

# Effect of aluminum doping on zinc oxide thin films grown by pulsed laser deposition for organic light-emitting devices

H. Kim<sup>a,\*</sup>, A. Piqué<sup>b</sup>, J.S. Horwitz<sup>b</sup>, H. Murata<sup>b</sup>, Z.H. Kafafi<sup>b</sup>, C.M. Gilmore<sup>a</sup>,  
D.B. Chrisey<sup>b</sup>

<sup>a</sup>*School of Engineering and Applied Science, George Washington University, 725 23rd St. NW, Washington DC 2005, USA*

<sup>b</sup>*Naval Research Laboratory, 4555 Overlook Ave, SW, Washington DC 2037, USA*

## Abstract

Transparent conducting aluminum-doped zinc oxide (AZO) thin films have been deposited on glass substrates by pulsed laser deposition. The structural, electrical and optical properties of these films were investigated as a function of Al-doping amount (0–4 wt.%) in the target. Films were deposited at a substrate temperature of 200°C in 0.67 Pa of oxygen pressure. It was observed that 0.8-wt.% of Al is the optimum doping amount in the target to achieve the minimum film resistivity and the maximum film transmission. For the 300-nm thick AZO film deposited using a ZnO target with an Al content of 0.8 wt.%, the electrical resistivity was  $3.7 \times 10^{-4} \Omega\text{-cm}$  and the average transmission in the visible range (400–700 nm) was 90%. The AZO films grown by PLD were used as transparent anodes to fabricate organic light-emitting diodes. The device performance was measured and an external quantum efficiency of 0.3% was measured at a current density of 100 A/m<sup>2</sup>. © 2000 Elsevier Science B.V. All rights reserved.

**Keywords:** Aluminum doped zinc oxide (AZO); Transparent conducting oxide (TCO); Pulsed laser deposition (PLD); Organic light emitting diodes (OLEDs)

## 1. Introduction

Recently, doped zinc oxide thin films have been widely studied for their use as transparent conducting electrode materials. Unlike the more commonly used indium tin oxide (ITO), zinc oxide (ZnO) is a non-toxic and inexpensive material. It is chemically (and thermally) stable under hydrogen plasma processes that are commonly used for the production of solar cells [1,2]. ZnO is a II–VI n-type semiconductor with a band gap of approximately 3.3 eV at room temperature and a hexagonal wurtzite structure [3]. Pure zinc oxide films are highly transparent in the visible range (400–700 nm) and have low electrical conductivity. However,

non-stoichiometric or impurity (group III elements) doped zinc oxide films have high electrical conductivities as well as high optical transparencies. Non-stoichiometric zinc oxide films have unstable electrical properties because the sheet resistance of ZnO films increases under either oxygen chemisorption and desorption [4] or heat treatment in vacuum or in inert gas at 400°C [5]. Unlike the non-stoichiometric ZnO films, impurity doped ZnO films show stable electrical and optical properties. Among the zinc oxide films doped with group III elements such as barium, aluminum, gallium and indium, aluminum-doped zinc oxide (AZO) films show the lowest electrical resistivity [6]. AZO films have low resistivity of  $2\text{--}4 \times 10^{-4} \Omega\text{-cm}$  [4,6–11], which is similar to that of ITO films [12–14]. AZO films are also wide band gap semiconductors ( $E_g = 3.4\text{--}3.9$  eV), which show good optical transmission in the visible and near-infrared (IR) regions. Due to these unique

\* Corresponding author. Tel.: +1-202-404-7989; fax: +1-202-764-5301.

E-mail address: hskim@ccf.nrl.navy.mil (H. Kim).

properties, AZO films have been used as transparent conducting electrodes in solar cells [1,2].

A number of thin film deposition techniques have been employed to grow AZO thin films including chemical vapor deposition (CVD) [2,7], magnetron sputtering [4,6,8], pulsed laser deposition (PLD) [9,10] and spray pyrolysis [15,16]. In comparison with other techniques, PLD provides several advantages. The composition of the films grown by PLD is quite close to that of the target, even for multicomponent targets. PLD films crystallize at lower substrate temperatures due to the high kinetic energies ( $> 1$  eV) of the atoms and ionized species in the laser-produced plasma [17]. In this paper, the effect of aluminum doping on structural, electrical and optical properties of AZO films deposited by PLD on glass substrates and the performance characteristics of organic light emitting diodes (OLEDs) with AZO anodes are reported.

## 2. Experimental

Films were deposited on glass substrates using a KrF excimer laser (Lambda Physics LPX 305, 248 nm and pulse duration of 30 ns). Details of the deposition system are described elsewhere [11–13]. The laser was operated at a pulse rate of 10 Hz. The laser beam was focused through a 50-cm focal length lens onto a rotating target at a  $45^\circ$  angle of incidence. The energy density of the laser beam at the target surface was maintained at  $2 \text{ J/cm}^2$ . The target-substrate distance was 4.7 cm. The target was a 2.5 cm diameter by 0.6-cm thick sintered oxide ceramic disk (98 wt.% ZnO and 2 wt.%  $\text{Al}_2\text{O}_3$ , 99.99% purity). All of the substrates were 7059 Corning glass cleaned in an ultrasonic bath with acetone and then methanol for 10 min. The deposition chamber was initially evacuated to  $1.3 \times 10^{-3} \text{ Pa}$  ( $1 \times 10^{-5}$  torr) and during deposition, oxygen background gas was introduced into the chamber to maintain the desired pressure.

The film thickness was measured by a stylus profilometer [KLA Tencor P-10]. The film resistivity was determined from the sheet resistance measurement by a four-point probe technique. Hall mobility and carrier density measurements were made using the Van der Pauw method [18] at room temperature. The optical transmission and reflectance measurements were made using a UV-visible-near infrared (IR) spectrophotometer (200–3200 nm) [Perkin-Elmer Lambda 9]. Refractive indices of the films were determined from the maxima and minima of the reflectance curve using the following relation:  $n \cdot d = k \cdot \lambda / 4$ , where  $n$  is the refractive index,  $d$  is the film thickness (nm),  $\lambda$  is the wavelength (nm) of the incident light, and  $k$  is the interference order (an odd integer for maxima and even integer for minima). X-Ray diffraction (XRD) (Rigaku rotating anode X-ray generator with  $\text{Cu K}_\alpha$  radiation)

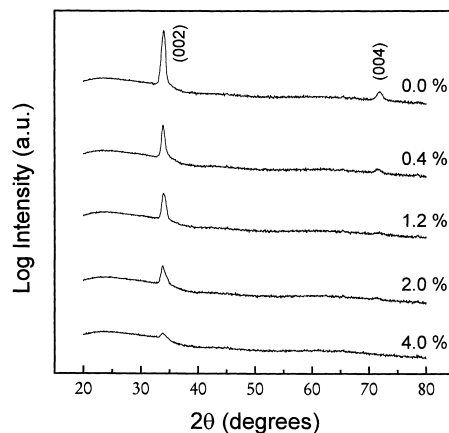


Fig. 1. X-Ray diffraction patterns for AZO films deposited on glass from targets with different Al contents. All films were deposited at  $200^\circ\text{C}$  in  $0.67 \text{ Pa}$  ( $= 5 \text{ mTorr}$ ) of oxygen. The film thickness was approximately 100 nm for all films.

was used to characterize the crystal structure of the films. The grain size ( $t$ ) is determined using the Scherrer formula;  $t = 0.9 \lambda / (B \cos \theta)$ , where  $\lambda$  is the X-ray wavelength,  $B$  is the corrected peak width and  $\theta$  is the Bragg diffraction angle [19]. Ultraviolet photoelectron spectroscopy (UPS) was used to measure the work function of the films.

## 3. Results and discussion

Doping of ZnO films with aluminum significantly affects the structural properties of the films. Fig. 1 shows the X-ray diffraction patterns for undoped ZnO and Al-doped ZnO films grown at  $200^\circ\text{C}$  in  $0.67 \text{ Pa}$  of oxygen pressure. Undoped ZnO film (0 wt.% in Fig. 1) was observed to be highly oriented with the c-axis orientation of (002) and (004). When the Al content in the targets increases, the (002) peak width becomes slightly broader, indicating that the grain size of the AZO films decreases with increasing the Al content in the targets. The calculated grain size of the undoped (0 wt.%) and Al-doped (0.8 wt.%) ZnO films was  $\sim 22$  and  $\sim 16$  nm, respectively. The c-axis lattice parameter, calculated from the XRD patterns for all AZO films, was in the range between 0.5247 and 0.5270 nm, which is larger than the JCPDS value<sup>1</sup> of 0.51948 nm for the ZnO powder. Since the radius (0.53 Å) of  $\text{Al}^{3+}$  is smaller than that (0.75 Å) of  $\text{Zn}^{2+}$ , the increase in the lattice parameters is probably due to the incorporation of Al ions in the interstitial positions [20]. This increase in lattice parameters may also be related to oxygen deficiency [13] and strain effect due to thermal expansion coefficient mismatch between the film ( $7 \times 10^{-6} / ^\circ\text{C}$ ) [21] and glass substrate ( $4.6 \times 10^{-6} / ^\circ\text{C}$ ).

<sup>1</sup>JCPDS Card No. 36-1451.

Doping of ZnO films with aluminum improves their electrical properties. Fig. 2 shows the typical variation of electrical resistivity ( $\rho$ ), carrier density ( $N$ ) and Hall mobility ( $\mu$ ) as a function of the Al content in the targets. The Al content was varied in the range from 0 to 4 wt.%. The substrate temperature was held at 200°C and the oxygen pressure was held constant at 0.67 Pa during deposition. The resistivity of the AZO films is found to initially decrease with increasing the Al content up to 0.8 wt.%. This decrease in resistivity is due to increase in free carrier concentrations as a result of the donor electrons from the Al dopant. This initial increase in carrier density in the AZO films was due to the substitutional incorporation of  $\text{Al}^{3+}$  ions at  $\text{Zn}^{2+}$  cation sites or incorporation of Al ions in interstitial positions. However, the resistivity of the AZO films, after reaching a minimum (at 0.8 wt.% of Al), gradually increases with a further increase in the Al content up to 4 wt.%. When the Al content in the target is greater than 0.8 wt.%, excess Al doping forms non-conducting  $\text{Al}_2\text{O}_3$  clusters in the films causing crystal disorder, which act as carrier traps rather than electron donors [2,15]. The excess Al-doping decreases the carrier concentration in the film and consequently increases the resistivity. It is further seen from Fig. 2 that the Hall mobility of the AZO films decreases with increasing the Al content. This decrease in mobility is also associated with the observed decrease in grain size of the AZO films. The decrease in grain size increases grain boundary scattering thus decreasing the mobility.

The Al-doping also affects the optical properties of the films such as transmittance ( $T$ ) and reflectance ( $R$ ). The transmittance and reflectance data were used to calculate absorption coefficients of the AZO films at different wavelengths. The absorption coefficient,  $\alpha$ , is given by the relation:

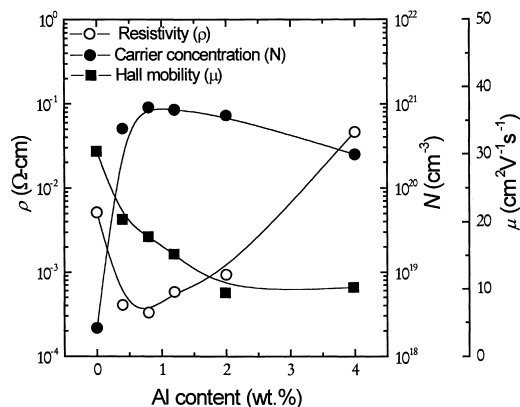


Fig. 2. Dependence of electrical resistivity ( $\rho$ ), carrier density ( $N$ ) and Hall mobility ( $\mu$ ) on the Al content in the targets used to deposit the AZO films ( $\sim 100$  nm). All films were deposited at 200°C in 0.67 Pa (= 5 mTorr) of oxygen.

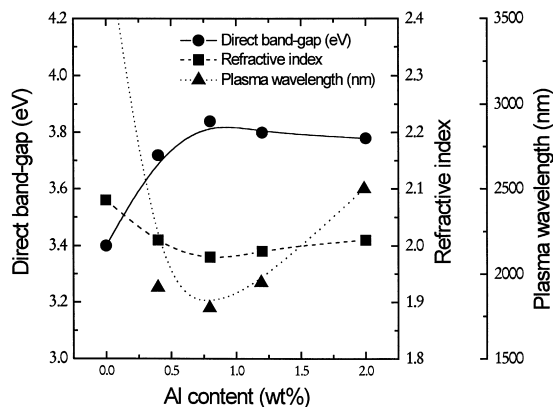


Fig. 3. Variation of direct band-gap ( $E_g$ ), refractive index ( $n$ ) and plasma wavelength ( $\lambda_p$ ) as a function of the Al content in the targets used to deposit the AZO films ( $\sim 100$  nm). All films were deposited at 200°C in 0.67 Pa of oxygen.

$$T = (1 - R)\exp(-\alpha d) \quad (1)$$

where  $d$  is the film thickness. The absorption coefficient data were used to determine energy gap,  $E_g$ , using the relation [22]:

$$\alpha h\nu \approx (h\nu - E_g)^{1/2}, \quad (2)$$

where  $h\nu$  is the photon energy. Fig. 3 shows the variation of the direct band-gap as a function of the target composition with the Al content for AZO films ( $\sim 100$  nm) deposited at 200°C and 0.67 Pa of oxygen. The value of  $E_g$  is observed to initially increase with increasing the Al content up to 0.8 wt.% and then become independent of Al-doping up to 2 wt.%. This initial increase in the band-gap is due to increase in free electron concentration in the films as a result of Al doping. This shift of the band-gap with the change in the carrier concentration can be explained by the B–M shift; the absorption edge shifts towards higher energy with an increase of carrier density [23,24]. However, for the films with Al doping above the critical level ( $\sim 0.8$  wt.%), the value of band-gap is slightly decreased due to a slight decrease in carrier concentration (see Fig. 2).

The Al-doping also affects the refractive index of the films as shown in Fig. 3. The refractive index is observed to decrease from 2.08 to 1.96 with an increase in Al doping from 0 to 0.8 wt.% and then slightly increase up to 2 wt.%. It is found that the refractive index is inversely related to the carrier concentration. The plasma wavelength (or cut-off wavelength) is defined at Transmittance = Reflectance where the dielectric-like visible transmittance equals to the metallic-like IR reflectance. Fig. 3 also shows that the plasma wavelength of the films decreases with increasing Al content up to 0.8 wt.% and then slightly increase up to 2 wt.%. The decrease in plasma wavelength is also related to

the increased carrier concentration in the films (see Fig. 2). The value of  $\lambda_p$  decreases with increasing Al content up to 0.8 wt.% due to the increase in carrier density ( $N$ ) shown in Fig. 2 and then increases again up to 2 wt.% due to a decrease in carrier density. Thus, the value of  $\lambda_p$  can easily be controlled by changing the carrier density through Al doping: The higher the carrier density, the lower is the value of  $\lambda_p$ . This result is in good agreement with Drude's theory [1,25].

Fig. 4 shows the optical transmittance and reflectance spectra for undoped (400 nm) and Al doped (300 nm) ZnO films grown at 200°C and 0.67 Pa of oxygen. For the undoped film, the transmittance is greater than 80% in the whole visible and near infrared (IR) region up to 3000 nm. For the Al-doped film (0.8 wt.%), the transmittance is greater than 85% in the visible range but decreases from 85 to 5% in the near IR region between 1200 and 3000 nm. This decrease in the transmittance in the near IR region is due to an increase in free electron concentration in the film as a result of Al doping. The plasma wavelength of 1600 nm is observed for the Al-doped ZnO film.

AZO films, grown by PLD from the 0.8 wt.%-Al doped-ZnO target, were used as anode materials for fabrication of OLEDs. The device structure used in this study is shown in the inset of Fig. 5. A 50-nm thick-hole transport layer (HTL) of *N,N'*-diphenyl-*N,N'*-bis (3-methylphenyl)1,1'-diphenyl-4,4'-diamine (TPD) was deposited on the AZO film by high vacuum vapor deposition. A 70-nm thick-electron transport/emitting layer (ETL/EML) of tris (8-hydroxyquinolinolato) aluminum (III) (Alq<sub>3</sub>) was then deposited on the TPD layer. The cathode contact deposited on top of the Alq<sub>3</sub> layer is an alloy of Mg/Ag (ratio = 12:1 and a thickness of 150 nm). Details of the fabrication of a similar device are described elsewhere [26]. The active area of the device is  $\sim 2 \times 2$  mm. The current density–voltage–luminance (J–V–L) data were taken

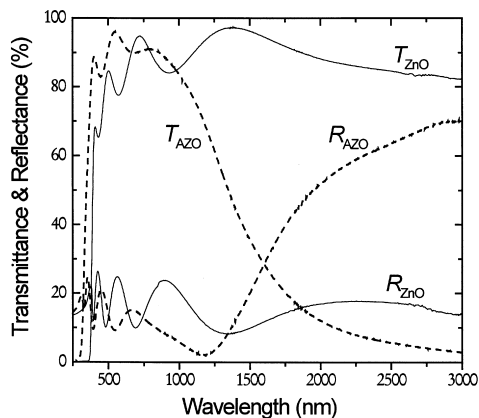


Fig. 4. Typical transmittance ( $T$ ) and reflectance ( $R$ ) spectra for the undoped ( $\sim 400$  nm) and 0.8-wt.% Al-doped ( $\sim 300$  nm) ZnO films grown at 200°C and 0.67 Pa of oxygen.

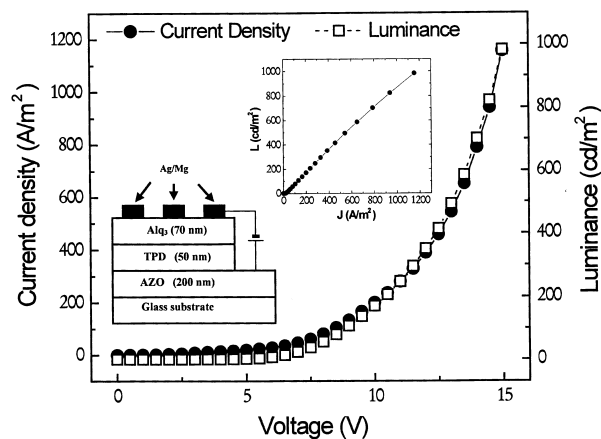


Fig. 5. Current density–voltage–luminance (J–V–L) characteristics of a heterostructure device schematically represented in the inset. An AZO film, grown by PLD at 200°C in 0.67 Pa of oxygen from the 0.8 wt.% Al-doped ZnO target, was used as an anode contact in this device.

(in a dry N<sub>2</sub> atmosphere) using a Keithley current/voltage source and a luminance meter (Minolta LS-110). Fig. 5 shows the J–V–L characteristics of an OLED with an AZO anode grown by PLD at 200°C and 0.67 Pa of oxygen. The JVL characteristics of the (AZO/TPD/Alq<sub>3</sub>/MgAg) diode show a typical diode behavior, with the current and power output observed only in the forward bias. A current density of  $\sim 100$  A/m<sup>2</sup> can be observed at  $\sim 8.4$  V in the device. A luminance of  $\sim 1000$  cd/m<sup>2</sup> was observed at 15 V and at a current density of  $\sim 1150$  A/m<sup>2</sup>.

As seen in Fig. 5, the luminance output from the device are linearly proportional to the current density output, in agreement with what is measured with a reference device fabricated with a commercially deposited ITO film (supplied by Planar America, USA). However, the external quantum efficiency measured from the AZO device was  $\eta_{\text{ext.}} \cong 0.3\%$  at  $\sim 100$  A/m<sup>2</sup>, which is lower than those measured ( $\eta_{\text{ext.}} \cong 1.0\%$ ) from the reference (ITO) device. This low efficiency is due to the low work function ( $\sim 4.0$  eV) of the AZO in comparison to that of commercial ITO (4.5–4.8 eV). Since the highest occupied molecular orbitals (HOMO) of the TPD lies  $\sim 5.5$  eV below vacuum, there is a significant energy barrier ( $\Delta E \approx 1.5$  eV) for hole injection from the AZO to the TPD layer.

#### 4. Conclusion

AZO films have been deposited by PLD on glass substrates. The structural, electrical and optical properties of the AZO films have been investigated as a function of Al-doping amount in the target. It was observed that 0.8-wt.% of Al is the optimum doping amount in the target to achieve the minimum film

resistivity and the maximum film transmission. The optical properties such as optical band gap, refractive index, plasma wavelength of AZO films were strongly affected by Al-doping amount. The optical band gap increased with an increase in carrier concentration as a result of Al-doping. As the Al-doping increased, the refractive index and the plasma wavelength decreased due to an increase in carrier concentration. For the 300-nm thick AZO film deposited from a 0.8-wt.%-Al-doped ZnO target, the electrical resistivity was  $3.7 \times 10^{-4} \Omega\text{-cm}$  and the average transmission in the visible range (400–700 nm) was 90%. These AZO films grown by PLD were used as transparent anodes to fabricate the OLEDs. The device performance was measured in the (AZO/TPD/Alq<sub>3</sub>/MgAg) diode and an external quantum efficiency of 0.3% was measured at a current density of 100 A/m<sup>2</sup>.

### Acknowledgements

This research was supported by office of Naval Research (ONR). We would like to thank Dr Eric Jackson for his help relating Hall effect measurements.

### References

- [1] H.L. Hartnagel, A.L. Dawar, A.K. Jain and C. Jagadish, *Semiconducting Transparent Thin Films*, Institute of Physics Publishing, Bristol and Philadelphia, 1995.
- [2] J. Hu, R.G. Gordon, *J. Appl. Phys.* 71 (1992) 880.
- [3] D.R. Lide, *Handbook of Chemistry and Physics*, 71st edn, CRC, Boca Raton, FL, 1991.
- [4] W. Gopel, U. Lampe, *Phys. Rev. B* 22 (1980) 6447.
- [5] T. Minami, H. Nanto, S. Takata, *Jpn. J. Appl. Phys.* 23 (1984) L280.
- [6] Y. Igasaki, H. Saito, *J. Appl. Phys.* 70 (1991) 3613.
- [7] S. Oda, H. Tokunaga, N. Kitajima, J. Hanna, I. Shimizu and H. Kokado, *Jpn. J. Appl. Phys.*, 24 (1085) 1607.
- [8] T. Minami, H. Sato, H. Natnto, S. Takata, *Jpn. J. Appl. Phys.* 24 (1985) L781.
- [9] A. Suzuki, T. Matsushita, N. Wada, Y. Sakamoto, M. Okuda, *Jpn. J. Appl. Phys.* 35 (1996) L56.
- [10] M. Hiramatsu, K. Imaeda, N. Horio, M. Nawata, *J. Vac. Sci. Technol. A* 16 (1998) 669.
- [11] H. Kim, J.S. Horwitz, A. Piqué, H. Murata, G.P. Kushto, R. Schlaf, Z.H. Kafafi, C.M. Gilmore, D.B. Chrisey, *Appl. Phys. Lett.* 76 (2000) 259.
- [12] H. Kim, A. Piqué, J.S. Horwitz, H. Mattoussi, H. Murata, Z.H. Kafafi, D.B. Chrisey, *Appl. Phys. Lett.* 74 (1999) 3444.
- [13] H. Kim, C.M. Gilmore, A. Piqué, J.S. Horwitz, H. Mattoussi, H. Murata, Z.H. Kafafi, D.B. Chrisey, *J. Appl. Phys.* 86 (1999) 6451.
- [14] H. Kim, J.S. Horwitz, A. Piqué, C.M. Gilmore, D.B. Chrisey, *Appl. Phys. A* 69 (1999) S447.
- [15] A.F. Aktaruzzaman, G.L. Sharma, L.K. Malhotra, *Thin Solid Films* 198 (1991) 67.
- [16] D. Goyal, P. Solanki, B. Maranthe, M. Takwale, V. Bhide, *Jpn. J. Appl. Phys.* 31 (1992) 361.
- [17] D.B. Chrisey, G.K. Hubler, *Pulsed Laser Deposition of Thin Films*, Wiley, New York, (1994) 327.
- [18] D.K. Schroder, *Semiconductor Material and Device Characterization*, John Wiley & Sons, New York, (1990).
- [19] B.D. Cullity, *Elements of X-ray Diffraction*, 2nd edn, Addison-Wesley, Reading, MA, 1978, p. 102.
- [20] W.D. Kingery, H.K. Bowen, D.R. Uhlmann, *Introduction to Ceramics*, Wiley, New York, (1976) 58.
- [21] M.-Y. Han, J.-H. Jou, *Thin Solid Films* 260 (1995) 58.
- [22] J. Tauc, R. Grigorovici, A. Vancu, *Phys. Stat. Sol.* 15 (1966) 627.
- [23] E. Burstein, *Phys. Rev.* 93 (1954) 632.
- [24] T.S. Moss, *Proc. Phys. Soc. London, Sect. B* 67 (1954) 775.
- [25] J.L. Vossen, *Phys. Thin Films* 9 (1977) 1.
- [26] H. Murata, C.D. Merritt, Z.H. Kafafi, *IEEE J. Sel. Topics Quant. Elec.* 4 (1998) 119.